

Role of Buoyancy in Fuel-Thermal-Stability Studies

V. R. Katta*

Systems Research Laboratories, Inc., Dayton, Ohio 45440
and

J. Blust,† T. F. Williams,‡ and C. R. Martel‡

University of Dayton Research Institute, Dayton, Ohio 45469

A unique methodology is used to investigate the effects of gravity on fuel flowing through the small-bore heated tubes that are often used in the study of fuel-thermal-stability characteristics. The copper block that houses the fuel tube (or test section) is located on a swivel, and experiments are conducted for different tube orientations, namely; horizontal, vertical with flow from bottom to top and vice versa. Results obtained for different fuel-flow rates and block temperatures are discussed. An axisymmetric, time-dependent numerical model is used to simulate the flow patterns in the test section. This model solves momentum, energy, species, and $k-\epsilon$ turbulence equations. The buoyancy term is included in the axial-momentum equation. Natural flow resulting from buoyancy was found to have a significant effect on heat transfer and oxygen consumption for fuel-flow rates up to 100 cc/min (Reynolds numbers up to 2.3×10^3). Flow instabilities were observed when the fuel was flowing downward in a vertically mounted test section. The effect of block temperature and flow rate on these instabilities was also studied.

Introduction

IN aircraft, before fuel is burned in the combustion chamber, it is used to cool several engine and airframe components as well as electronic equipment.¹ The bulk-fuel temperature and the high wall temperature of these components lead to degradation of the fuel (i.e., chemical decomposition of fuel to form gums and solids that cause fouling of fuel nozzles and heat exchangers). Several laboratory experiments of the flowing^{2,3} and static⁴ type have been designed to study the thermal stability of jet fuel. Temperature is usually treated as an effective parameter⁵ for correlating experimentally obtained data and fuel behavior in aircraft. Recent studies^{6,7} have indicated strong involvement of certain species such as dissolved oxygen and hydroperoxides in the fouling process. In order to extend the findings derived from these laboratory experiments to real aircraft fuel systems, a thorough understanding of the experimental data is needed. Knowledge of the temperature and species distributions within the test section of an experiment is essential for analyzing the complex data on deposition.

In commonly used flowing experiments^{2,3,5,6} in fuel-thermal-stability studies, fuel is passed continuously through a long, small-bore heated tube (test section). The tube is heated by either passing electric current through the tube wall² (constant heat flux) or using an external, constant-temperature heat source.^{3,5,6} The test sections are mounted either horizontally^{3,5} or vertically,² with fuel flowing from top to bottom or vice versa. In each of these situations, the forced laminar or turbulent convection is altered in a different way by the free (or natural) convective flow.

During heating, the fluid near the wall is warmer and, therefore, lighter than the bulk fluid in the core. As a consequence, in a horizontally mounted tube, two upward currents flow along the side walls and, by continuity, the heavier fluid near the center of the tube flows downward. This establishes two spiral vortices that are symmetrical about a vertical meridional

plane.⁸ This combined forced and natural convective flow causes the heat-transfer coefficient to be higher than that predicted using laminar-flow assumptions. The secondary motion with the uniform-temperature boundary condition develops to a maximum intensity and then diminishes to zero as the temperature gradients in the fuel decrease. If the tube is placed vertically, then the fuel near the side wall is accelerated along the tube length for the bottom-to-top forced flow and decelerated for the top-to-bottom forced flow. The greater shear between the core and the near-wall fluid in the former case could establish ring vortices that are symmetric about the axis of the tube as a result of the Kelvin-Helmholtz-type instability.⁹ Similar vortices could develop in the latter case (top-to-bottom forced flow) also, resulting from the Taylor instability.¹⁰ As these vortices enhance mixing, the heat-transfer coefficient increases above its expected laminar value, but remains less than its turbulent value. Although the effects of natural flow on convective flow have been addressed in the past,¹¹ those studies were limited to relatively large cross sections (>1 cm) and, hence, are not relevant for the small-bore tubes used in fuel-thermal-stability studies.

In the present study, the effects of free convection on forced flow in a long, small-bore tube for different test-section orientations were investigated experimentally and theoretically using a time-dependent mathematical model. The tube was heated with a constant-temperature copper block. An aviation fuel, Jet A, was used as the flow media. The results are characterized by the Reynolds and Grashof numbers.

Experimental Arrangement

Several fuel-thermal-stability experiments were conducted on a single-pass, flowing fuel system known as the Phoenix rig.³ Figure 1 is a schematic diagram of the rig that consists of two test sections, two copper blocks (one for heating and the other for cooling), a fuel-supply system, filters, and several measuring instruments. Small-bore stainless steel tubes, 0.3175 cm o.d., 0.216 cm i.d., and 55.9 cm in length, are used as the test sections. The internal surface of the tube is not electropolished, having a roughness of 0.2–0.38 μm . The heating block consists of a copper cylinder measuring 45.7 cm in length and 7.6 cm in diam. The copper cylinder is split lengthwise in two halves, with each section containing a full-length cartridge heater. A lengthwise groove on the flat face of each

Received March 7, 1994; revision received June 29, 1994; accepted for publication June 30, 1994. Copyright © 1994 by the American Institute of Aeronautics and Astronautics, Inc. All rights reserved.

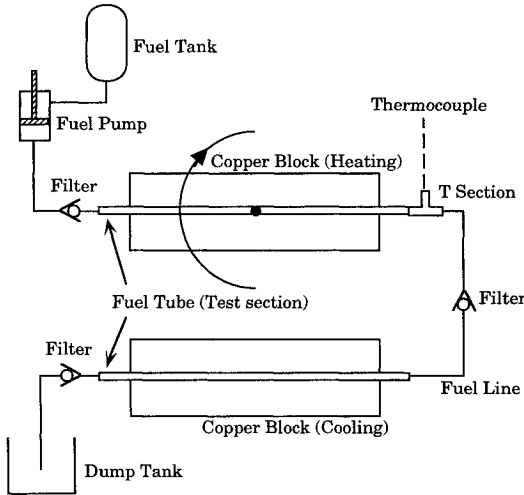
*Senior Engineer, Research Applications Division. Member AIAA.

†Graduate Student, Research Institute. Student Member AIAA.

‡Research Engineer, Research Institute.

Table 1 Source terms and transport coefficients appearing in governing equations

Φ	Γ^Φ	S^Φ
u	$\mu + \mu_t$	$-\frac{\partial p}{\partial z} + \frac{\partial}{\partial z} \left(\Gamma^u \frac{\partial u}{\partial z} \right) + \frac{\partial}{\partial r} \left(\Gamma^u \frac{\partial v}{\partial z} \right) + \frac{\Gamma^u}{r} \frac{\partial v}{\partial z} + \rho g$
v	$\mu + \mu_t$	$-\frac{\partial p}{\partial r} + \frac{\partial}{\partial z} \left(\Gamma^v \frac{\partial u}{\partial r} \right) + \frac{\partial}{\partial r} \left(\Gamma^v \frac{\partial v}{\partial r} \right) + \frac{\Gamma^v}{r} \frac{\partial v}{\partial r} - 2\Gamma^v \frac{v}{r^2}$
k	$\mu + \frac{\mu_t}{\sigma_k}$	$G - \rho \varepsilon$
ε	$\mu + \frac{\mu_t}{\sigma_\varepsilon}$	$C_1 G \frac{\varepsilon}{k} - C_2 \rho \frac{\varepsilon^2}{k}$
h	$\frac{k}{c_p} + \frac{\mu_t}{\sigma_h}$	0
Y_i	$\rho D_i + \frac{\mu_t}{\sigma_{Y_i}}$	\dot{w}_i

**Fig. 1** Schematic diagram of single-pass, flowing system (Phoenix Rig) used for studies of fuel-thermal-stability characteristics.

cylinder section was provided in order that a 0.3175-cm-diam hole would form to house the test section when the copper-block sections were clamped together. The cooling block is designed similarly, except that it is not provided with cartridge heaters.

Only the central 45.7-cm section of each stainless steel tube was clamped inside the heated copper block, leaving the 5.1-cm-long tube sections on both ends unheated. However, both the end sections of the tube were insulated by wrapping them using fiberglass. The end of the fuel tube was connected to a T section for measuring the bulk fuel temperature T_{BE} . Several thermocouples were also connected to the fuel tube in order to profile the tube-outer-wall temperature T_w . The temperature of the copper block T_{CB} was maintained at the desired value using an on-line-monitoring computer. In order to avoid vaporization of fuel the system was pressurized to 350 psi.

The heated copper block was mounted on a swivel system to permit its rotation up to 270 deg from the horizontal position. This would allow horizontal (0 deg), vertical with flow-up (90 deg), and vertical with flow-down (270 deg) configurations. The second copper block is generally used to study the fuel-thermal-stability characteristics during the cooldown process; however, in the present investigation of the flow characteristics, it was used as a means to cool fuel prior to its return to the dump tank.

Mathematical Model

Fluid motion inside the tubular test section is assumed to be axisymmetric. The time-dependent Navier-Stokes equations along with the turbulent-energy, species-conservation,

and enthalpy equations that are solved in the z - r cylindrical coordinate system are as follows¹²:

$$\frac{\partial \rho}{\partial t} + \frac{\partial \rho u}{\partial z} + \frac{\partial \rho v}{\partial r} + \frac{\rho v}{r} = 0 \quad (1)$$

$$\begin{aligned} \frac{\partial \rho \Phi}{\partial t} + \frac{\partial \rho u \Phi}{\partial z} + \frac{\partial \rho v \Phi}{\partial r} &= \frac{\partial}{\partial z} \left(\Gamma^\Phi \frac{\partial \Phi}{\partial z} \right) \\ &+ \frac{\partial}{\partial r} \left(\Gamma^\Phi \frac{\partial \Phi}{\partial r} \right) - \frac{\rho v \Phi}{r} + \frac{\Gamma^\Phi}{r} \frac{\partial \Phi}{\partial r} + S^\Phi \end{aligned} \quad (2)$$

Here, ρ , u , and v are the density and the axial and radial velocity components, respectively. Equation (2) represents different conservation equations, depending on the variable assigned to Φ . The source terms S^Φ and the transport coefficients Γ^Φ associated with each of these equations are given in Table 1. The gravity term is added to the axial-momentum equation to simulate the flow-up or flow-down in a vertically mounted tube.

In Table 1, μ , k , and c_p are the viscosity, thermal conductivity, and specific heat of the fuel, respectively, and μ_t is the turbulent viscosity incorporated through use of the k - ε turbulence model. The variables p , h , k , and ε are the pressure, enthalpy, and turbulence kinetic energy and its dissipation, respectively, and σ is the turbulent Prandtl number (or Schmidt number) associated with a specific transport equation. Y_i , w_i , and D_i are the mass fraction, rate of production, and diffusion coefficient of the i th species, respectively. The other variables and constants appearing in the table are defined below:

$$G = \mu_t \left\{ 2 \left[\left(\frac{\partial u}{\partial z} \right)^2 + \left(\frac{\partial v}{\partial r} \right)^2 + \left(\frac{v}{r} \right)^2 \right] + \left(\frac{\partial v}{\partial z} + \frac{\partial u}{\partial r} \right)^2 \right\}$$

$$\mu_t = C_\mu \rho k^2 / \varepsilon$$

$$C_1 = 1.47, \quad C_2 = 1.92, \quad \text{and} \quad C_\mu = 0.09$$

$$\sigma_k = 1.0, \quad \sigma_\varepsilon = 1.3, \quad \sigma_h = 1.0, \quad \text{and} \quad \sigma_{Y_i} = 1.0$$

The transport properties, enthalpy, and density at a given temperature are obtained from the curve fits developed for the available Jet-A fuel data.¹³ The governing equations are discretized utilizing a hybrid scheme,¹⁴ which is a second-order central differencing scheme everywhere, but changes to a first-order upwind scheme when the local cell-Reynolds number becomes greater than 2. The finite difference form of the governing equations are solved sequentially adopting an implicit approach¹² and a uniform grid system having 31 points in the radial direction and 101 points in the axial direction. This grid density was found to be yielding results that are only weakly sensitive to the further grid refinement. While

flat velocity profiles were used at the tube entrance as initial conditions, values of the flow variables at the tube exit plane were obtained by extrapolating the data at the interior grid points. For the turbulent-flow calculations, wall functions¹⁵ have been used to determine the gradients of the flow variables near the wall boundary. Due to the destructive procedure adopted in the experiments to measure carbon deposition, low-cost fuel tubes with medium surface finish were used. The surface roughness could influence the growth of the boundary layer in the fuel tube; however, to simplify the mathematical modeling, it is not taken into account.

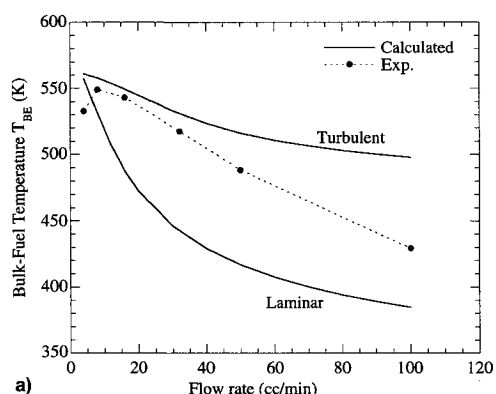
The chemical-kinetics models described by Krazinski et al.¹⁶ and Katta et al.¹⁷ are capable of predicting carbon deposition on the tube wall. However, since the present study was limited to the effects of buoyancy on heat transfer and oxygen depletion, the deposit-formation chemistry was not considered. The oxygen consumption is governed by the single irreversible reaction



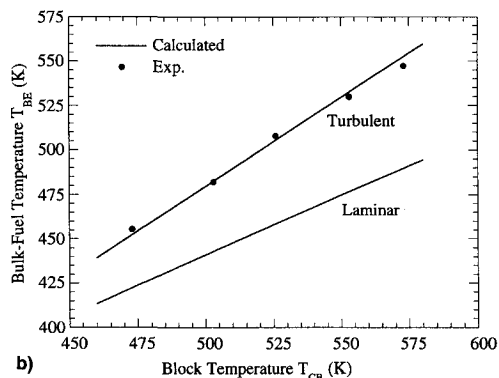
The reaction rate for the above equation is assumed to be governed by an Arrhenius expression and of zeroth order with respect to the reactants. The pre-exponential (2.53×10^{13} mole/m³/s) and activation energy (32 kcal/mole) were determined for the Jet A fuel used by Katta et al.¹⁷ The same values were selected for the present simulations since the Jet A fuel used in these studies is only slightly different from that of Katta et al.¹⁷

Results and Discussion

The bulk temperature measured at the exit of the horizontal fuel tube for different flow rates is shown in Fig. 2. The copper-block temperature T_{CB} was 573 K. The temperature of the fuel before entering the tube was 292 K. The Reynolds



a)



b)

Fig. 2 Comparison of predicted and measured bulk fuel temperature in horizontal position at exit of fuel tube: a) for different flow rates, block temperature is 573 K and b) for different block temperatures, flow rate is 16 cc/min.

number (based on the diameter of the fuel tube and the fuel properties at the end of the tube) obtained for the highest flow rate of 100 cc/min was $\sim 2.3 \times 10^3$, which suggests that the flow inside the test section should be laminar for all flow rates used in this experiment. Note that the Reynolds numbers calculated based on the fuel properties at the inlet are an order of magnitude lower than those obtained at the end of the tube. As expected, the measured bulk-fuel temperature decreased with the flow rate. However, at a very low flow rate of 4 cc/min, the bulk-fuel temperature is lower than that measured at 8 cc/min. This is believed to be resulting from the insufficient insulation provided between the end of the heated section and the thermocouple location.

Calculations were initially made by neglecting gravity term in the axial-momentum equation (Table 1) and by assuming a laminar-type flow inside the test section, and the results are shown in Fig. 2a. The bulk-fuel temperature predicted for different flow rates is significantly lower than the measured value. Based on the facts that 1) the present calculations employed widely accepted temperature-dependent density and transport coefficients¹³ for a Jet-A fuel, 2) the code used for these simulations was well tested in the past for its accuracy in predicting the wall and fuel temperatures in similar heating systems but operating at higher flow rates, and 3) the pressure (350 psi) and the copper-block temperature (<573 K) adopted in the present experiments guarantee a single-phase flow in the fuel tube; one might question, in light of the differences noted between the theory and experiment, the use of laminar-flow assumption. The higher temperatures (compared to the laminar predictions) in the experiment then could be due to some kind of flow turbulence. To investigate the possibility of flow being turbulent inside the tube, calculations were made assuming a turbulent flow in the test section. However, a very low level of fluctuating velocity ($\sim 1\%$ of the mean) was used at the tube entrance.

The exit bulk temperatures obtained under the assumption of turbulent flow are also compared with the experimental data in Fig. 2a. It should be noted from this figure that when the flow rate is low (<40 cc/min), the turbulent simulation predicts the T_{BE} more accurately than the laminar simulation. A similar observation was made from calculations obtained for an experiment in which the flow rate was fixed (16 cc/min) and the block temperature was varied. Both the computed and the measured data are plotted in Fig. 2b. Close agreement between the measured values and those predicted by the turbulent-flow simulation is evident. It should also be noted from Fig. 2a that as the flow rate increases, the measured values approach the calculated laminar data. This raises two questions: 1) is the flow at lower flow rates (or Reynolds numbers) turbulent and, if so, 2) why does it become laminar at higher flow rates. These issues will be addressed both theoretically and experimentally in the following sections.

Influence of Buoyancy

The density of the fuel changes significantly with temperature (840 kg/m³ at room temperature and 650 kg/m³ at 500 K), which gives rise to considerable buoyancy force on the fuel near the tube wall. As the test section is mounted horizontally, the buoyancy force acts in the direction normal to the fuel flow. It is known that such a buoyancy force on the fluid passing between two horizontally mounted parallel plates gives rise to Taylor instabilities,¹⁰ which, in turn, develop into large vortices. However, in the case of circular tubes, the Taylor instabilities result in a three-dimensional flow. In both situations, the induced flow normal to the heated walls increases the heat transfer coefficient.

Since the inside diameters of tubes used in fuel-thermal-stability experiments are usually smaller than 0.5 cm, one might intuitively expect that the large three-dimensional vortices break down into smaller ones, yielding a flow pattern that resembles a turbulent flow. The induced free flow (or

natural flow) is significant when the convective flow (or flow rate) is low and becomes less significant as the flow rate increases. This results in laminarization of the flow in the tube. Therefore, the fluid flow in a horizontally mounted, heated tube can be characterized as a turbulent flow when the flow rate is small, approaching a laminar flow as the flow rate increases. At much higher flow rates (Reynolds numbers above 2.3×10^3), the convective flow itself becomes turbulent and the buoyancy forces become negligible. The data shown in Fig. 2a support these concepts on free flow in horizontally mounted, small-bore circular tubes. The bulk exit temperature follows turbulent-flow predictions initially and, as the flow rate is increased, it shifts toward laminar-flow predictions. Neither the exit bulk temperature nor the wall temperature in the experiment exhibited fluctuations that would indicate that large-scale vortices similar to those observed in large-bore tubes¹¹ are not present in the present experiment.

Although temperature predictions for a horizontally mounted heated tube suggest that the flow within the test section is turbulent (induced by buoyancy), evidence could not be obtained in this enclosed system using the recently developed visualization techniques¹⁸ because the tube bore is too small and tube itself is embedded in a copper block. Also, the dynamics of the flow were not captured by the numerical simulation since the mathematical formulation was based on the assumption that the flow is axisymmetric. In order to gain a better understanding of the importance of buoyancy in these flows, different experiments were designed. The problem associated with three dimensionality of the flow was eliminated by mounting the test section vertically. In this configuration the buoyancy forces are parallel to the flow direction; hence, buoyancy does not induce three dimensionality in the flow. The flow rates and block temperatures used were identical to those in Fig. 2; however, the fuel temperature was different at the entrance of the fuel tube. Usually, the fuel was driven from bottom to top. The heater block in the experiment is fabricated in such a way that it can be rotated counterclockwise 90 deg, and clockwise by 180 deg for studying the horizontal and flow-down conditions, respectively.

Experiments and numerical simulations for different test-section orientations were made to investigate the changes in heat-transfer characteristics. The predicted and measured bulk fuel temperatures at the exit of the fuel tube for different flow rates are shown in Fig. 3. The block temperature was fixed at a value of 573 K. For each flow rate, four different calculations were performed, using the following assumptions concerning the flowfield: 1) flow is turbulent and buoyancy forces in the axial direction are negligible—to simulate the flow inside the horizontally mounted tube; 2) laminar flow without buoyancy terms—to provide an estimate for the effects of natural flow in this system; 3) laminar flow and buoyancy forces act along the convective flow—to simulate the vertically upward flow and; 4) laminar flow on which buoyancy acts in the direction opposite that of the convective-flow direction—to represent the vertically downward flow.

For all flow rates considered in this study (2–100 cc/min), the first three assumptions yielded steady-state flows. However, the vertically downward flow calculations resulted in large fluctuations in the bulk temperature at the exit of the fuel tube. This was found to result from the convective motion of the large-scale vortices that developed inside the heated section of the tube. The formation of these vortices and their characteristics will be discussed later. Results obtained with the above four models are presented in Fig. 3 along with the respective experimental data.

As expected, for all flow rates the horizontal configuration yielded the highest bulk temperatures at the end of the test section. Calculations made under the assumption of turbulent flow yielded accurate predictions for these flows up to a flow rate of 50 cc/min. For higher flow rates the measurements are shifted toward the laminar predictions. As seen from Fig. 3,

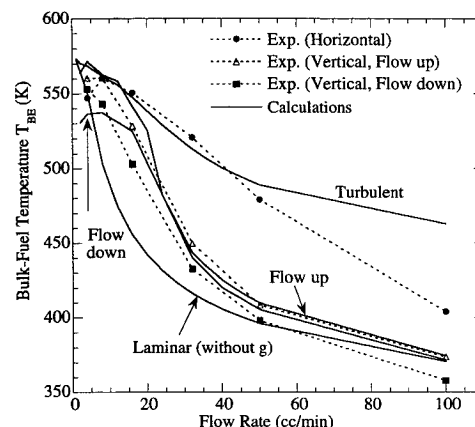


Fig. 3 Computed and measured bulk fuel temperature at exit of fuel tube for different test-section orientations ($T_{CB} = 573$ K).

the agreement between the measured and calculated bulk temperatures for the vertically upward flow is very good for all flow rates considered. This suggests that the highest fuel flow rate (or Reynolds number) used in these heated-tube experiments, i.e., 100 cc/min, does not produce turbulent flow. Therefore, the turbulent-type flows observed for the lower flow rates in the horizontally mounted tubes result from free convection in the radial direction rather than due to the forced convection in the axial direction.

A comparison of the bulk temperatures predicted for laminar flows (Fig. 3) with and without the gravity term in the governing equations indicates that the influence of free convection on forced convection decreases with flow rate and is almost negligible at a flow rate of 100 cc/min. This in conjunction with the earlier discussion on the flow-up case in the vertically mounted configuration indicates that, as the flow rate increases, the flow inside a horizontally mounted, heated tube approaches laminar conditions. This phenomenon was also observed in buoyancy-dominated combustions and is often referred to as "relaminarization."¹⁸

For a given flow rate, the vertically mounted configuration with fuel flowing downward yielded the lowest bulk temperatures at the tube exit (cf. Fig. 3). This means that heat transfer occurs in a very inefficient way when free (or natural) convection opposes forced convection. Since the simulations for this case were unsteady in nature, the T_{BE} profile shown in Fig. 3 was obtained by time-averaging the data. For flow rates greater than or equal to 32 cc/min, the calculated T_{BE} for flow-down case closely followed that of the flow-up case.

Temperature Distribution Obtained with Different Models

Experiments conducted at different block temperatures and fuel-flow rates have indicated similar behavior, as discussed in the previous section. However, when the heated tube was placed in a vertical position and with fuel flowing downward, the exit bulk temperatures showed strong fluctuations for certain flow and block-temperature conditions. The periodic nature of these oscillations gave the first indication about the Taylor instabilities developing inside the small-bore heated tubes that are generally used for fuel thermal studies. To understand the growth and nature of these instabilities, flow simulations were made using the four models described previously with different block temperatures and flow rates.

Temperature distributions for a flow rate of 32 cc/min and a block temperature of 573 K predicted by the previously discussed models are shown in Fig. 4. Eleven equally spaced isotherm contours between 290–590 K are plotted in each case. Velocity fields associated with the four cases of Fig. 4 are shown in Figs. 5a–5d, respectively. A low turbulent kinetic energy was used at the inlet for the turbulent flow simulation. However, as the fuel temperature increased (and

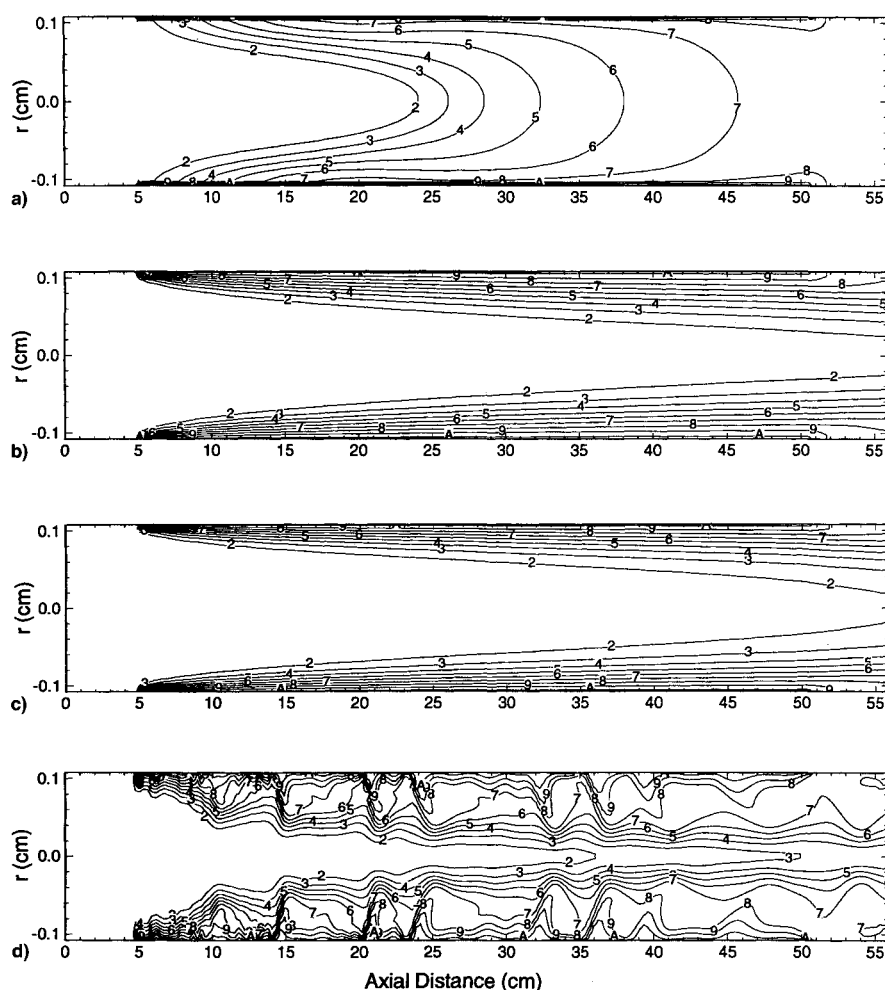


Fig. 4 Temperature distributions predicted for fuel flow rate of 32 cc/min using assumptions of a) turbulent flow, b) laminar flow with no gravity, c) laminar flow with buoyancy force acting in same direction of forced flow and, d) laminar flow with buoyancy force acting in opposite direction of forced flow. Eleven equally spaced contours are plotted between 290–590 K.

density decreased) with axial distance, the velocity and, hence, the turbulent kinetic energy increased. This introduced higher heat flux into the fuel from the tube wall, as indicated by the higher fuel temperature in Fig. 4a. As discussed earlier, this turbulent simulation globally represents the flow inside a horizontally mounted heated tube.

The gravitational force was neglected in the simulation of Figs. 4b and 5b. Under the laminar-flow assumption, the thermal layer (region between contours A and 2) became thinner (cf. Fig. 4b), and most of the fuel at the tube center was cold, having a temperature very near that of the incoming fuel. The fuel velocity within the thermal layer increased (cf. Fig. 5c) due to the natural flow in the flow-up case. As a result, the higher temperature contours were pushed towards the wall (cf. Figs. 4b and 4c). However, as seen from Fig. 3, the bulk fuel temperature in this case is greater than that of the laminar flow. The buoyant acceleration of the hot fuel along the heated wall entrained more cold fuel into the thermal layer, leading to an increase in the heated-fuel flow along the wall and, hence, to a higher bulk fuel temperature. This acceleration did not initiate any flow instabilities (Kelvin-Helmholtz type), and the entire flow remained steady state (Fig. 5c).

When the buoyancy force was opposite to the forced-flow direction (flow-down configuration), several vortices developed along the heated wall (Figs. 4d and 5d) and the flow became unsteady. Unlike the vortices in other buoyancy-dominated flows such as diffusion flames^{18,19} and flow over a heated plate,²⁰ the vortices in these heated tubes are noncoherent and irregular in size and shape. This is due, in part, to the very large aspect ratio (length-to-diameter of ~ 200) associ-

ated with the small-bore tubes used in this study. Note that the scales in the axial and radial directions in Figs. 4 and 5 are not the same. Nevertheless, the thermal layer resulting from the presence of vortices is significantly increased. The convective motion of these vortices led to fluctuations in bulk temperature at the exit of the fuel tube. Interestingly, the fuel velocity in the thermal layer is reduced in this case (Fig. 5d) when compared to that in the other three cases (Figs. 5a–5c). Due to continuity of mass, fuel velocity near the center of the tube in the flow-down case has increased appreciably. The higher cold-fuel flow at the tube center resulted in a bulk-fuel-exit temperature that is less than that obtained in flow-up case (Fig. 3).

Predicted and measured bulk-fuel temperatures as functions of time are plotted in Fig. 6. The Fourier analysis of the data shows that the computed flow is fluctuating with frequencies near 0.5 and 3.0 Hz. On the other hand, the dominating frequency of the measured fluctuations is ~ 0.4 Hz. In the numerical simulations the bulk exit temperature was calculated by integrating the mass-weighted temperature at the exit of the tube at a given instant of time. The bulk-fuel temperature in the experiment was obtained by passing the fuel through a “T section,” which was assumed to provide an equilibrium temperature through mixing. However, this procedure could easily destroy small vortices and fail to reproduce the higher frequencies associated with small-scale vortices. Considering the differences in the data-acquisition techniques and the assumption made concerning tube surface roughness, the calculations seem to predict the magnitude and lower frequency of the temperature fluctuations reasonably well.

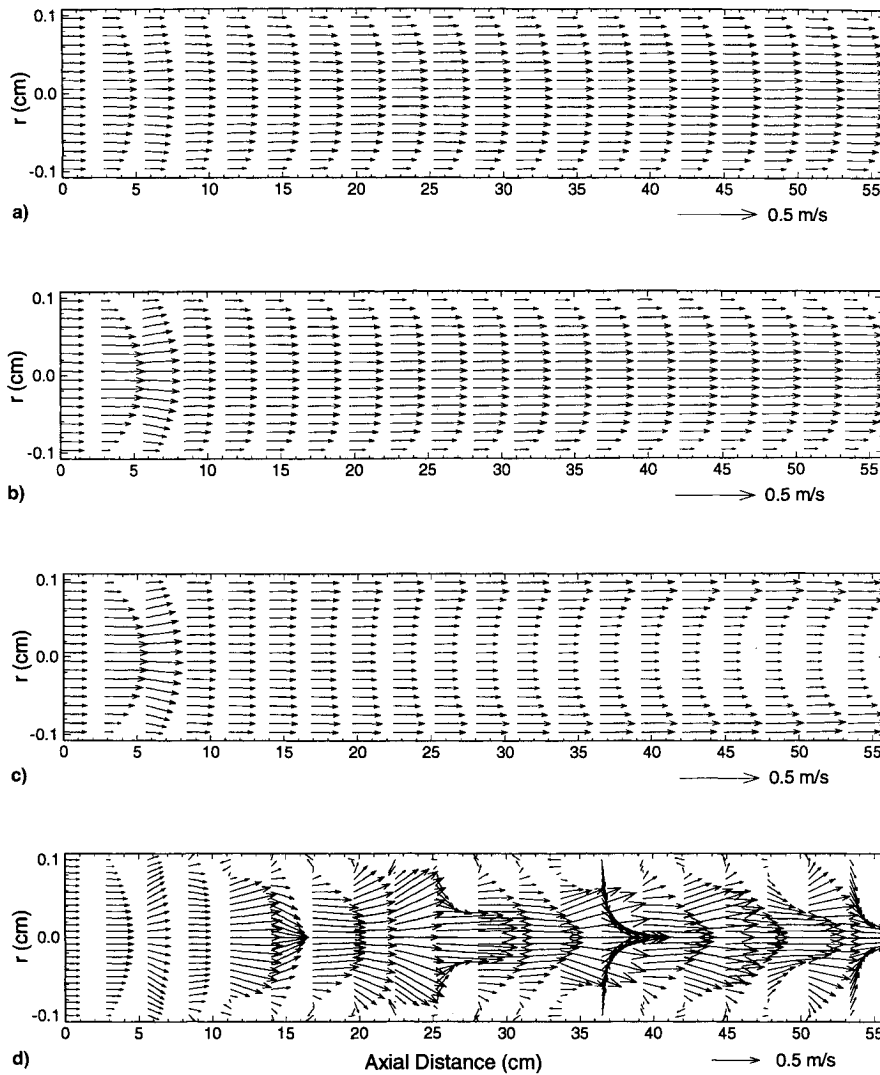


Fig. 5 Velocity fields corresponding to the four calculations of Fig. 4.

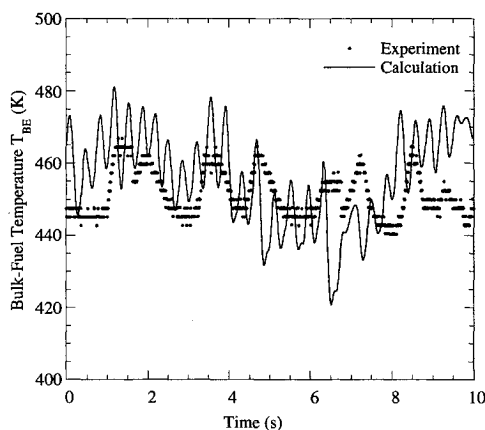


Fig. 6 Computed and measured temperature fluctuations obtained for fuel flow rate of 32 cc/min and block temperature of 573 K in vertically mounted heated tube with fuel flowing from top to bottom.

Effect of Block Temperature on Instabilities

Both the simulations and the experiments demonstrated that instabilities can develop in a vertically mounted heated tube when the fuel is flowing from top to bottom. The effect of block temperature on these instabilities was studied by maintaining the flow rate constant at 32 cc/min. The computed temperature distributions inside the fuel tube obtained with

the flow-down model are plotted in Fig. 7. Results for block temperatures of 473, 513, and 553 K are shown here. For the three block temperatures, the initial thermal layer became unstable. However, at $T_{CB} = 473$ K (Fig. 7a), the instabilities seem to be organized and dampened within 5.0 cm of the tube, and the remainder of the flow became laminar. No fluctuations were observed in the exit bulk temperature, which was steady at a value of 357 K. As the block temperature was increased, the hot fuel along the wall penetrated farther upstream into the preheater section. The stronger buoyancy force in the cases of $T_{CB} = 513$ and 553 K led to destruction of the orderliness of the vortices. Large-scale vortices formed through vortex merging, and the entire thermal layer became unsteady. For a block temperature of 513 K, only the large-scale vortices survived at the tube exit, and the bulk-fuel temperature there fluctuates at ~ 0.9 Hz only. On the other hand, at $T_{CB} = 553$ K both the small- and large-scale vortices are passing through the tube. The exit bulk temperature displays fluctuations similar to those observed for $T_{CB} = 573$ K (Figs. 4d and 6). It may be speculated that for higher block temperatures, the thermal layer becomes turbulent.

Weakening of flow instabilities at lower block temperatures is in qualitative agreement with the observations made in the experiments. The bulk-fuel temperatures measured at the tube exit were found to fluctuate when the block temperature was higher than 560 K. This cutoff temperature compares favorably with that of 513 K obtained from the simulations.

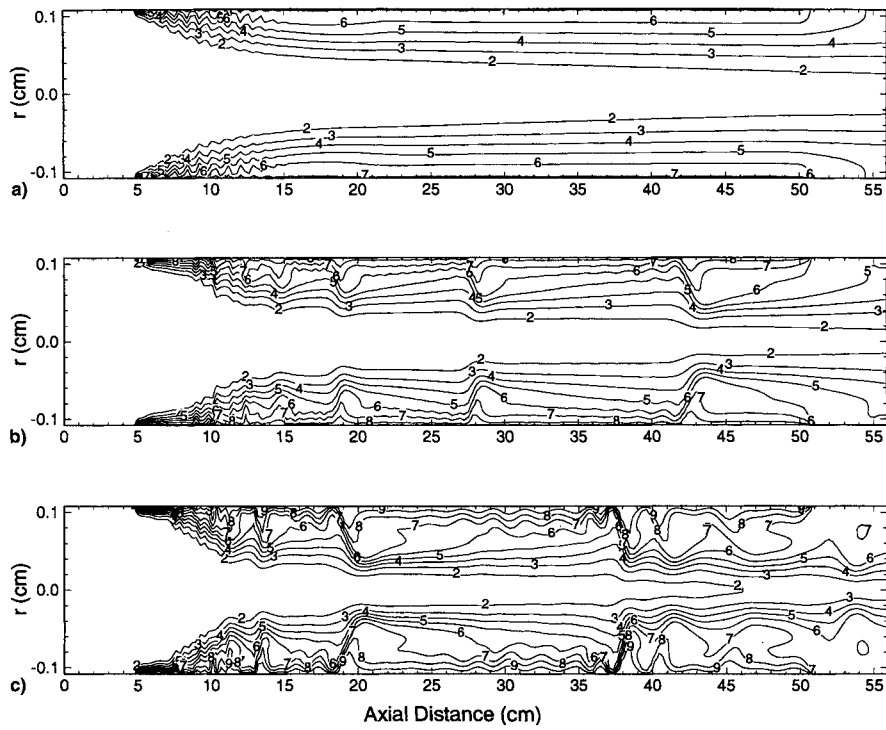


Fig. 7 Temperature distributions obtained for block temperatures of a) 473, b) 513, and c) 553 K in vertically mounted heated tube with fuel flowing from top to bottom. Fuel-flow rate is 32 cc/min.

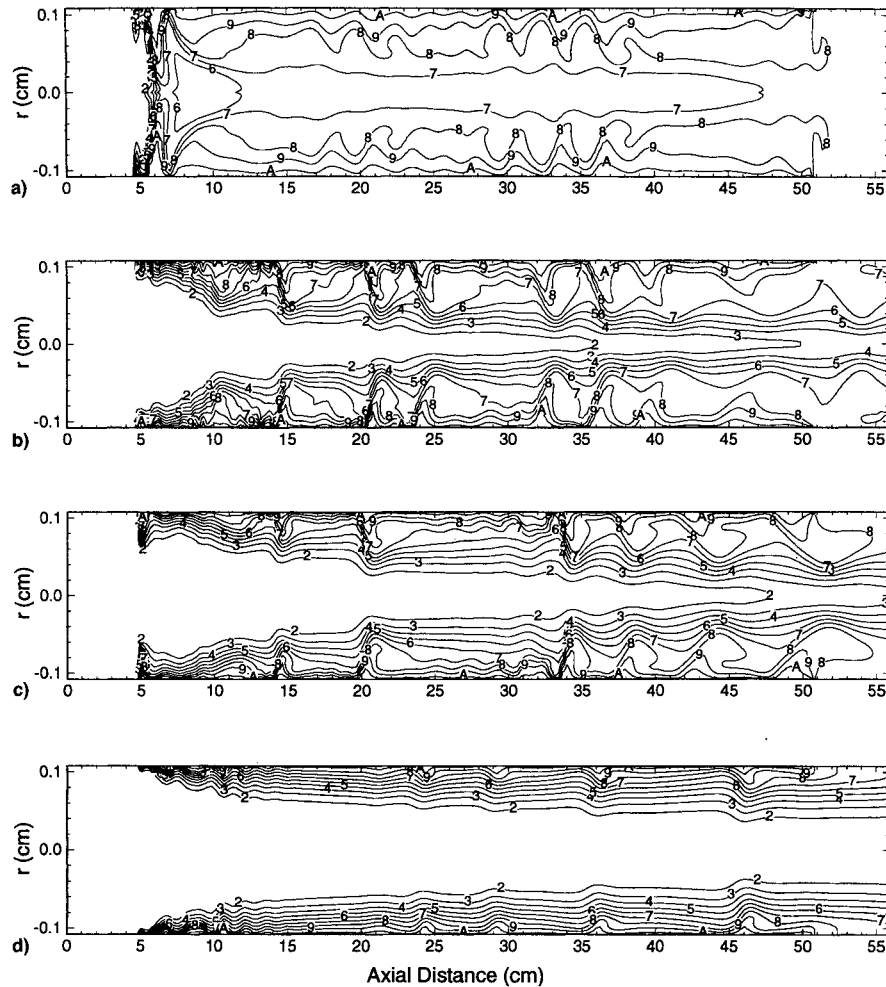


Fig. 8 Temperature distributions obtained for fuel-flow rates of a) 8, b) 32, c) 50, and d) 100 cc/min in vertically mounted heated tube with fuel flowing from top to bottom. Block temperature is 573 K.

Effect of Flow Rate on Instabilities

From Figs. 2 and 3 it can be observed that the influence of gravity on the convective flow in a heated tube decreases with flow rate. In order to understand how the flow rate modifies the instabilities in the flow-down configuration, simulations were made for different fuel flow rates. Instantaneous temperature fields obtained for flow rates of 8, 32, 50, and 100 cc/min are shown in Figs. 8a–8d, respectively. Copper-block temperature in all these cases was 573 K. Two interesting observations may be made from these figures. First, the thermal-layer thickness decreases, and secondly, the instabilities become weaker with increased flow rate. The instabilities in the case of the 8-cc/min flow rate grew rapidly to the scale of the tube radius. Figure 8a indicates that the fuel toward the end of the tube is approaching an equilibrium value. The well mixedness of the fuel inside the tube gave rise to weak temperature fluctuations, although large-scale vortices are continuously passing at the tube exit. Stronger fluctuations in the bulk fuel temperature are observed at the tube exit for flow rates of 32 and 50 cc/min (Figs. 8b and 8d). The weaker instabilities in the 100-cc/min flow-rate case gave rise to weak oscillations in the bulk-fuel temperature, confirming the re-laminarization of the flow.

Similar behavior between the bulk-fuel temperature at the exit and the flow rate was observed while conducting flow-down experiments in the vertically mounted heated tube. These results are plotted in Fig. 9 in the form of standard deviations for the measured bulk-temperature fluctuations for different flow rates. The Reynolds and Richardson numbers obtained based on the tube i.d. and length, respectively, and the fuel properties at the inlet are given along with the flow rates. The block temperature in these calculations was maintained at 573 K. The average bulk-fuel temperature at the tube exit and the Grashof number are also plotted in Fig. 9. It is clear from this plot that fluctuations in the bulk-fuel temperature were strong when the flow rate was between 16–47 cc/min. At flow rates higher than 47 cc/min, the forced flow dominated the buoyancy-induced natural flow that resulted in reduced fluctuations in temperature.

It is common to characterize the flow in terms of whether it is dominated by buoyancy based on Grashof number. Figure 9 indicates that in the flow-down cases, the flow becomes buoyancy dominated when the Grashof number is $>6.0 \times 10^{11}$. However, the Grashof number does not correctly char-

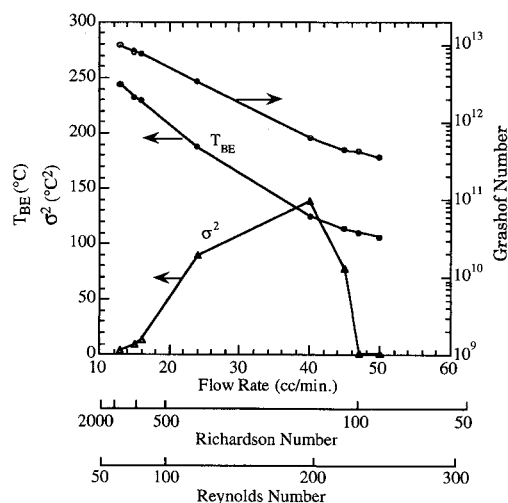


Fig. 9 Measured average and standard deviation of fuel bulk temperature and associated Grashof numbers for different flow rates in vertically mounted heated tube with fuel flowing from top to bottom. Block temperature is 573 K.

acterize the flow oscillations that result from the natural flow. Fluctuations in temperature are observed only when the Grashof number is $<9.0 \times 10^{12}$ and $>6.0 \times 10^{11}$.

Effect of Buoyancy on Oxygen Consumption

Fouling in heated tubes is strongly coupled to the consumption of dissolved oxygen, which, in turn, is dependent on the temperature distribution. The global-chemistry model developed for predicting deposition in heated tubes was successfully used in the Phoenix-rig experiments.³ The same model was used in the present study to understand the influence of buoyancy on oxygen consumption.

Concentration of dissolved oxygen in the fuel before it enters the heated tube was assumed to be 50 ppm, which represents the level in the air-saturated fuel. Calculations were made using the four mathematical models discussed previously under the same conditions used with reference to Fig. 4. The remaining oxygen and the temperature of the bulk fuel (obtained by mass-weighted integration) at different axial locations are plotted in Fig. 10. The turbulent-flow simulation that represents the horizontal configuration of the tube predicts a significant amount of oxygen present throughout the tube. Interestingly, from Fig. 10, it may be noted that the fuel was heated to the highest temperature in this simulation. This is in contrast to the general belief on fuel oxidation that higher bulk fuel temperature leads to a greater consumption of dissolved oxygen. The inconsistency of the lower oxygen consumption for higher bulk-fuel temperature results from 1) turbulent conditions transport heat readily in the radial direction and, thus, do not generate a high-temperature thermal boundary layer along the heated wall and 2) the higher velocity near the wall that reduces the residence time necessary for chemical reaction to occur.

The reduced velocity in the thermal layer in the laminar simulation (Fig. 5b) yielded high consumption of oxygen along the tube wall. The buoyant flow along the wall in the vertical, flow-up configuration increased the entrainment of fuel into the thermal layer. The oxygen consumption was initially decreased compared to that of the laminar flow (Fig. 10) up to $z \approx 35$ cm because of the increased velocity (or reduced residence time), and then increased due to entrainment. A significant amount of oxygen is consumed in the vertically mounted heated tube when the fuel is flowing from top to bottom

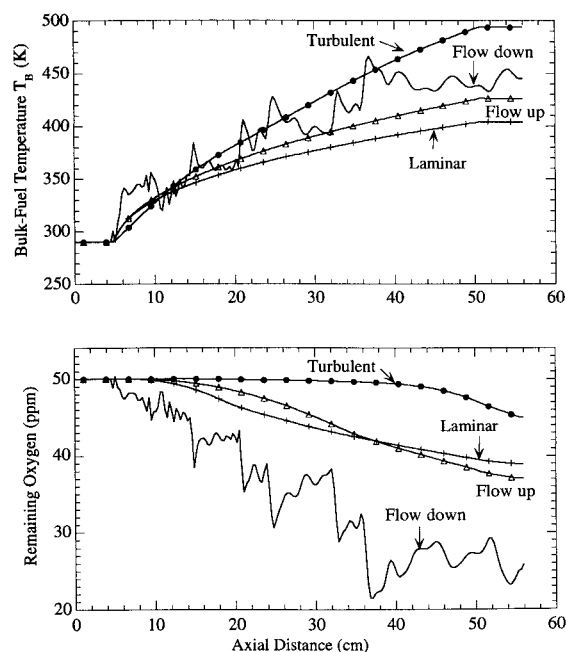


Fig. 10 Remaining oxygen and bulk fuel temperature at different axial locations predicted by different models. Fuel-flow rate and block temperature are 32 cc/min and 573 K, respectively.

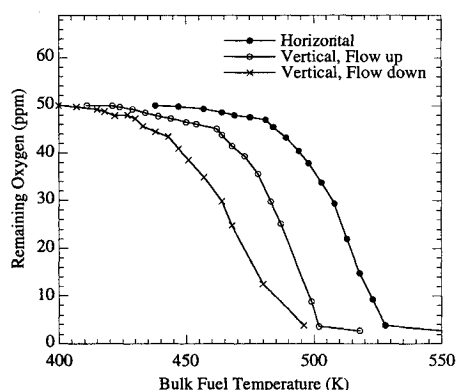


Fig. 11 Remaining oxygen vs bulk fuel temperature measured with different orientations of heated tube. Flow rate is 16 cc/min.

bottom as a result of the increased residence time in the thermal layer. In fact, consumption of oxygen is maximum in this case compared to the other three simulations.

The oxygen consumption in the Jet A fuel was measured using on-line instrumentation of Phoenix rig³ for the three tube orientations. Data in the form of remaining oxygen vs bulk fuel temperature at the exit of the heated tube is plotted in Fig. 11. All these measurements were made for a flow rate of 16 cc/min and by varying the copper-block temperature. Figure 11 shows that for a given value of T_{BE} , consumption of dissolved oxygen is the highest in a vertically mounted tube with fuel flowing from top to bottom and the lowest when the tube was placed horizontally. This qualitatively supports the predictions discussed previously. Note, Fig. 3 indicates that for the given fuel-flow rate and block-temperature, the vertically mounted tube with fuel flowing down yields the lowest bulk fuel temperature at the tube exit.

It is known that deposition on the wall increases with consumption of oxygen.^{3,6,16,17} Therefore, it may be expected that maximum deposition occurs on the tube walls in a vertically mounted, heated tube when the fuel is flowing top to bottom and minimum deposition occurs in a horizontally oriented fuel tube. Due to the nonmonotonic behavior of deposition with temperature (i.e., deposition initially increases and then decreases with fuel temperature^{2,3}), the vertically mounted, heated tube with flow-down configuration may not represent the worst scenario for all block temperatures. Global-reaction models proposed such as those in Refs. 16 and 17 are capable of predicting the deposition by taking into account the fluid-dynamics and heat-transfer effects on the fuel flow. Future studies with theoretically and experimentally obtained deposition data for different fuel-tube orientations may be useful in validating such global-chemistry models.

Conclusions

The flow structure in a small-bore heated tube was studied experimentally and theoretically. It was found that buoyancy has a significant impact on the temperature field. Because of the difficulties associated with extending currently available flow-visualization techniques to small-bore tubes, the influence of natural flow on forced flow was investigated by conducting unique experiments and performing time-dependent numerical simulations for different heated-tube orientations. Experiments yielded the highest bulk-fuel exit temperature when the test-section was mounted horizontally and the lowest in a vertically mounted test-section with fuel flowing from top to bottom. Numerical simulations have reproduced most of the observed features.

The following conclusions are drawn from the comparative experimental and numerical studies made in this article.

1) When the fuel is flowing in a horizontally mounted, small-bore tube, the flow pattern is more turbulent in nature

at very low Reynolds numbers and becomes laminar in nature as the Reynolds number increases to 2300.

2) It is hypothesized that the buoyancy forces normal to the force-flow direction increase mass and heat transport, develop three dimensionality, and, thereby, render the flow turbulent.

3) An axisymmetric code with the $k-\epsilon$ turbulent model is found to yield reasonable predictions for horizontal flow. However, a more realistic simulation of buoyancy dominated fuel flow in a horizontally mounted, heated tube should be performed using a three-dimensional code.

4) Vertically mounted, heated tube with fuel flowing from bottom to top is observed to yield axisymmetric, laminar flows up to a flow rate of 100 cc/min in the 0.3175-cm-diam tubes considered in this study.

5) Fuel flowing from top to bottom in a vertically mounted, heated tube develops flow instabilities when the flow rate is moderate.

6) Oxygen consumption is found to be minimum in the horizontal case and maximum when the fuel is flowing from top to bottom in a vertically mounted tube.

Acknowledgments

This work was supported by the U.S. Air Force under Contracts F33615-90-C-2033 and F33615-92-C-2207. The authors would like to thank the principal investigators, Larry Goss and Dilip Ballal, and the Air Force Technical monitor, Mel Roquemore, for supporting this work and participating in the stimulating discussions.

References

- Koff, B. L., "The Next 50 Years of Jet Propulsion, the Global Anniversary of Jet Powered Flight: 1939-1989," Dayton and Cincinnati AIAA Meeting, Dayton, OH, Aug. 1989.
- Marteney, P. J., and Spadaccini, L. J., "Thermal Decomposition of Aircraft Fuels," *Journal of Engineering for Gas Turbines and Power*, Vol. 108, Oct. 1986, pp. 648-653.
- Ballal, D. R., Byrd, R. J., Heneghan, S. P., Martel, C. R., Williams, T. F., and Zabarnick, S., "Combustion and Heat Transfer Studies Utilizing Advanced Diagnostics: Fuel Research," Wright Lab. TR WR-TR-92-2112, Wright-Patterson AFB, OH, Nov. 1992.
- Jones, E. G., and Balster, W. J., "Application of a Sulphur-Doped System to the Study of Thermal Oxidation of Jet Fuels," International Gas Turbine and Aeroengine Congress and Exposition, American Society of Mechanical Engineers, Paper 92-GT-122, Cologne, Germany, June 1992.
- Chin, J. S., and Lefebvre, A. H., "Influence of Flow Conditions on Deposits from Heated Hydrocarbon Fuels," International Gas Turbine and Aeroengine Congress and Exposition, American Society of Mechanical Engineers, Paper 92-GT-114, Cologne, Germany, June 1992.
- Jones, G., Balster, W. J., and Post, M. E., "Degradation of a Jet-A Fuel in a Single-Pass Heat Exchanger," International Gas Turbine and Aeroengine Congress and Exposition, American Society of Mechanical Engineers, Paper 93-GT-334, Cincinnati, OH, May 1993.
- Heneghan, S. P., and Zabarnick, S., "Oxidation of Jet Fuels and the Formation of Deposits," *Fuel*, Vol. 73, No. 1, 1994, p. 35.
- Mori, Y., Futagami, K., Tokuda, S., and Nakamura, M., "Forced Convective Heat Transfer in Uniformly Heated Horizontal Tubes," *International Journal of Heat and Mass Transfer*, Vol. 9, No. 5, 1966, pp. 453-463.
- Brown, G. L., and Roshko, A., "On Density Effects and Large Structure in Turbulent Mixing Layers," *Journal of Fluid Mechanics*, Vol. 64, No. 4, 1974, pp. 775-816.
- Busse, F. H., "Transition to Turbulence in Rayleigh-Benard Convection," *Hydrodynamic Instabilities and the Transition to Turbulence*, edited by H. L. Swinney and J. P. Gollub, Springer-Verlag, Berlin, 1981.
- Mori, Y., and Futagami, K., "Forced Convective Heat Transfer in Uniformly Heated Horizontal Tubes," *International Journal of Heat and Mass Transfer*, Vol. 10, No. 12, 1967, pp. 1801-1813.
- Katta, V. R., and Roquemore, W. M., "Numerical Method for Simulating Fluid-Dynamic and Heat-Transfer Changes in Jet-Engine

Injector Feed-Arm Due to Fouling," *Journal of Thermophysics and Heat Transfer*, Vol. 7, No. 4, 1993, pp. 651-660.

¹³Nixon, A. C., Ackerman, G. H., Faith, L. E., Henderson, H. T., Ritchie, A. W., Ryland, L. B., and Shryne, T. M., "Vaporizing and Endothermic Fuels for Advanced Engine Application: Part III, Studies of Thermal and Catalytic Reactions, Thermal Stabilities, and Combustion Properties of Hydrocarbon Fuels," Air Force Aero Propulsion Lab., AFAPL-TR-67-114, Pt. III, Vol. II, Wright-Patterson AFB, OH, 1967.

¹⁴Spalding, D. B., "A Novel Finite Difference Formulation for Difference Expressions Involving Both First and Second Derivatives," *International Journal for Numerical Methods in Engineering*, Vol. 4, No. 4, 1972, pp. 551-559.

¹⁵Launder, B. E., and Spalding, D. B., "The Numerical Computation of Turbulent Flows," *Computer Methods in Applied Mechanics and Engineering*, Vol. 3, No. 2, 1974, pp. 269-289.

¹⁶Krazinski, J. L., Vanka, S. P., Pearce, J. A., and Roquemore, W. M., "A Computational Fluid Dynamics and Chemistry Model for

Jet Fuel Thermal Stability," *Journal of Engineering for Gas Turbines and Power*, Vol. 114, Jan. 1992, pp. 104-110.

¹⁷Katta, V. R., Jones, E. G., and Roquemore, W. M., "Development of Global-Chemistry Model for Jet-Fuel Thermal Stability Based on Observations from Static and Flowing Experiments," *Fuels and Combustion Technology for Advanced Aircraft Engines*, Paper 19, AGARD, Loughton, Essex, England, UK, Sept. 1993, pp. 19-1-19-11 (AGARD CP-536).

¹⁸Roquemore, W. M., Chen, L.-D., Goss, L. P., and Lynn, W. F., "Structure of Jet Diffusion Flames," *Turbulent Reactive Flows, Lecture Notes in Engineering*, edited by R. Borghi and S. N. B. Murthy, Vol. 40, Springer-Verlag, Berlin, 1989, pp. 49-63.

¹⁹Chen, L.-D., Roquemore, W. M., Goss, L. P., and Vilimpoc, V., "Vorticity Generation in Jet Diffusion Flames," *Combustion Science and Technology*, Vol. 77, Nos. 1-3, 1991, pp. 41-57.

²⁰Holman, J. P., Gartrell, H. E., and Soehngen, E. E., "An Interferometric Method of Studying Boundary Layer Oscillations," *Journal of Heat Transfer*, Vol. 82, Aug. 1960, pp. 263, 264.